Force Balance and Stability of Toroidal Helical Coil with Circular Cross Section*)

Takayuki HABUCHI, Hiroaki TSUTSUI, Shunji TSUJI-IIO and Ryuichi SHIMADA
Tokyo Institute of Technology, Tokyo 152-8550, Japan

(Received 8 December 2010 / Accepted 7 April 2011)

Stability and force equilibrium of toroidal helical coil with circular cross section were investigated. In this paper, we derived and calculated equations for equilibrium of toroidal helical coil based on an axisymmetric surface current model. The helical coil, which is modulated in such a way that a magnetic surface coincides with the coil surface, can reduce overturning force generated by electromagnetic forces. We analyzed the stability of the toroidally modulated helical coil and confirmed that this modulated configuration is held in equilibrium while it is unstable. This condition means the minimum inductance condition. Moreover, we formulated the relationships between electromagnetic forces and stresses acting on toroidal helical coil with circular cross section, and we compared the stress distributions calculated by the equations with those from finite element method (FEM) analysis.

Keywords: stress analysis, FEM, helical coil, force balance, modulated coil

DOI: 10.1585/pfr.6.2405150

1. Introduction

Stronger magnetic fields improve the performance of magnetic confinement fusion devices. However, strong magnetic field causes huge electromagnetic forces, and an increase in cost becomes a problem. We investigated helical coils that reduce stresses caused by electromagnetic forces. The coils are based on the concept of balancing the hoop force generated by central solenoid (CS) and the centering force caused by toroidal field coils (TFCs) [1–7]. The coils were designed to be wound to make a magnetic surface coincide with the coil surface, thus overturning forces generated on the coils are minimized. The coils can generate strong magnetic field even when the device size is small. Superconducting magnetic energy storage (SMES) by this coil concept was studied, under the condition that coils were not fixed, the maximum operating current was up to 86% of the critical current and the maximum magnetic field achieved was 6.1 T [8]. However, it was difficult to raise further, and it was attributed to the movement of coil conductors.

In this paper, we investigated the stability of toroidally modulated helical coil with circular cross section based on an axisymmetric surface current model. And we formulated the relationships between electromagnetic forces and stresses acting on toroidal helical coil with circular cross section.

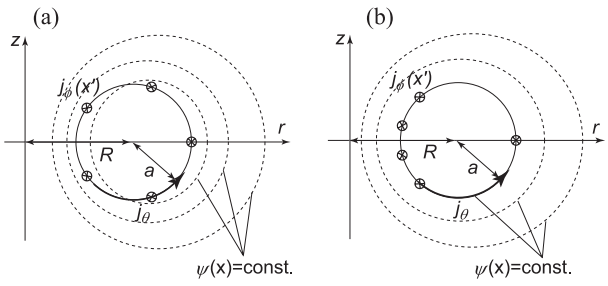

Fig. 1 Illustrations of coil current distribution depicted by solid line and magnetic surfaces indicated by dotted lines under the condition that magnetic surfaces intersect coil surface (a), and a magnetic surface coincides with the coil surface (b).

2. Toroidally Modulated Helical Coil

When a helical coil is modulated in such a way that a magnetic surface coincides with the coil surface, the overturning force generated by electromagnetic forces can be reduced. This magnetic configuration was developed from an axisymmetric surface current model. Poloidal magnetic flux Ψ at $x = (R, z)$ is given by

$$\Psi(\boldsymbol{x}) = \oint G(\boldsymbol{x}, \boldsymbol{x'}) j_\phi(\boldsymbol{x'}) \mathrm{d}s', \tag{1}$$

where the contour integral is done on the current surface, and j_ϕ is toroidal surface current density, and G is the Green function expressed by using complete elliptic integral of first kind $K(k)$ and complete elliptic integral of second kind $E(k)$ as follows,

author's e-mail: habuchi@nr.titech.ac.jp

*) This article is based on the presentation at the 20th International Toki Conference (ITC20).

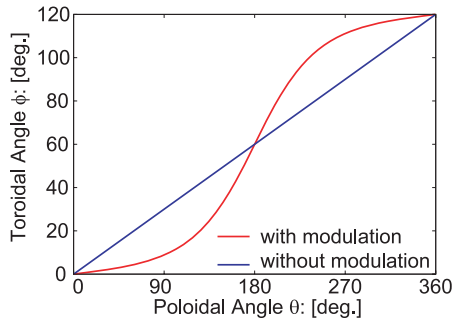

Fig. 2 Relationships between poloidal angle θ and toroidal angle ϕ. Blue line shows the pitch of helical coil without modulation and red one shows that of the modulated coil.

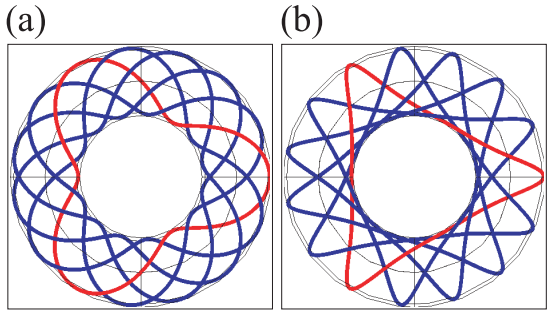

Fig. 3 Plan view of current paths without pitch modulation (a), and with modulation (b). Red line indicates one current path.

$$G(\boldsymbol{x},\boldsymbol{x}') = 2\frac{\mu_0\sqrt{rr'}}{k}\left(\frac{1-k^2}{2}K(k) - E(k)\right), \tag{2}$$

$$k = \sqrt{\frac{4rr'}{(r+r')^2+(z+z')^2}}. \tag{3}$$

On a magnetic surface, poloidal magnetic flux Ψ is constant:

$$\Psi(\boldsymbol{x}) = \Psi_0 = \text{const.} \tag{4}$$

The magnetic surface expressed by Eq. (4), in general, intersects the coil surface as shown in Fig. 1 (a). The configuration that a magnetic surface coincides with the coil surface can be achieved by distributed toroidal current density j_ϕ as shown in Fig. 1 (b). Toroidal magnetic field is also generated by poloidal surface current density j_θ,

$$j_\theta = \frac{I_\theta}{2\pi}\frac{1}{r}. \tag{5}$$

The current path on the torus is determined by current density components, j_ϕ and j_θ. When j_ϕ/j_θ is constant, the path on the θ-ϕ plane is straight and the pitch angle is also constant. The pitch angle is modulated for the distributed j_ϕ configuration whose current shell coincides with a magnetic surface as shown in Fig. 2. Figure 3 shows current paths of toroidally helical coil without pitch modulation (a) and with modulation (b). Although the current path of a real helical coil system is non-axisymmetric as shown in Fig. 3, we adapt an axisymmetric shell current model, thus the shell current density and magnetic field are also axisymmetric.

3. Stability of Modulated Helical Coil

In this section, we investigate the stability of toroidally modulated helical coil with circular cross section, and it is assumed that a magnetic surface coincides with a torus shell and the coil current distributes on the shell surface. Poloidal magnetic energy U is expressed by

$$\begin{aligned} U &= \oint\frac{1}{2}\Psi j_\phi \mathrm{d}s \\ &= \frac{1}{2}\oint \mathrm{d}s \oint \mathrm{d}s' j_\phi(\boldsymbol{x})G(\boldsymbol{x},\boldsymbol{x}')j_\phi(\boldsymbol{x}'), \end{aligned} \tag{6}$$

with poloidal magnetic flux Ψ. Since poloidal magnetic flux Ψ generated by the modulated coil is expressed by Eq. (4), the variation in the magnetic energy is written as follows:

$$\begin{aligned} \delta U &= \frac{1}{2}\oint \mathrm{d}s \oint \mathrm{d}s'\delta j_\phi G j_\phi + \frac{1}{2}\oint \mathrm{d}s \oint \mathrm{d}s' j_\phi G \delta j_\phi \\ &= \frac{1}{2}\Psi_0\left(\oint \delta j_\phi \mathrm{d}s + \oint \delta j_\phi \mathrm{d}s'\right). \end{aligned} \tag{7}$$

Here, we choose δj_ϕ satisfying

$$\oint \delta j_\phi \mathrm{d}s = 0 \tag{8}$$

with a constant current source. Since the right-hand side of Eq. (7) is zero, the modulated coil is in equilibrium. Next, $\delta^2 U$ is written as follows:

$$\delta^2 U = \frac{1}{2}\oint \mathrm{d}s \oint \mathrm{d}s'\delta j_\phi G \delta j_\phi \geq 0, \tag{9}$$

since the Green function G is positive definite and symmetrical quadratic form. Consequently, when the modulation changes under a current conservation condition, the inductance of coil increases. The electromagnetic force F on a coil system in constant-current operation is obtained as follows [9]:

$$F = \nabla U. \tag{10}$$

Therefore the increment in $\delta^2 U$ expressed as Eq. (9) indicates that the modulated coil is an unstable equilibrium against any axisymmetric displacement on the torus shell surface.

4. Electromagnetic Force on Helical Coil

4.1 Formulation of force-balanced system

In this section, we include intersected magnetic fields and extended the equilibrium equation [10] of torus shell with a circular cross section under the condition that a magnetic surface coincides with coil surface. In this paper, uniform stiffness of the torus shell is assumed. Choosing

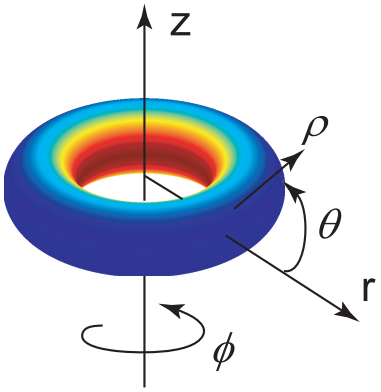

Fig. 4 Semi-toroidal coordinate system (ρ, ϕ, θ).

semi-toroidal coordinate system (ρ, ϕ, θ) shown in Fig. 4, equilibrium equations for the helical coil are obtained as follows:

$$-\frac{1}{ar}\left\{r\sigma_{\theta\theta}+(r-R)\,\sigma_{\phi\phi}\right\}=f_{\rho}, \tag{11}$$

$$\frac{1}{ar}\frac{\mathrm{d}}{\mathrm{d}\theta}\left(r\sigma_{\theta\phi}\right)=arf_{\phi}, \tag{12}$$

$$\frac{\sin\theta}{r}\left\{\sigma_{\phi\phi}-\frac{\mathrm{d}}{\mathrm{d}r}\left(r\sigma_{\theta\theta}\right)\right\}=f_{\theta}. \tag{13}$$

Here $\sigma_{\phi\phi}$ and $\sigma_{\theta\theta}$ are normal stresses in the θ and ϕ directions, respectively, $\sigma_{\theta\phi}$ is shearing stress, f_{θ}, f_{ϕ} and f_{ρ} are electromagnetic forces per unit volume in the θ, ϕ and ρ directions, respectively. Denoting major and minor radii by R and a, respectively, r is given by $r = R + a\cos\theta$. The solutions to this simultaneous differential equations are given as follows:

$$\sigma_{\theta\theta}=\frac{u}{r(r-R)}, \tag{14}$$

$$\sigma_{\phi\phi}=\frac{f_{\rho}ar}{r-R}-\frac{u}{(r-R)^2}, \tag{15}$$

using u obtained by

$$u(r)=\int_{R}^{r}\left\{af_{\rho}(r')r'-\frac{f_{\theta}(r')r'\,(r'-R)}{\sqrt{1-\frac{(r'-R)^2}{a^2}}}\right\}\mathrm{d}r'. \tag{16}$$

Shearing stress $\sigma_{\theta\phi}$ becomes zero at $\theta = \pi/2$ where the moment of the electromagnetic overturning force vanishes, and given by

$$\sigma_{\theta\phi}=\frac{1}{r}\int_{\pi/2}^{\theta}raf_{\phi}\mathrm{d}\theta. \tag{17}$$

When a magnetic surface generated by the helical coil intersects its coil surface, f_{ϕ} acts on the coil and the coil is subjected to a shearing stress $\sigma_{\theta\phi}$ as expressed by Eq (17). Moreover, in such a case, f_{θ} also acts on the coil, and f_{θ} contributes to normal stresses $\sigma_{\theta\theta}$ and $\sigma_{\phi\phi}$ as expressed by Eqs. (14)-(16).

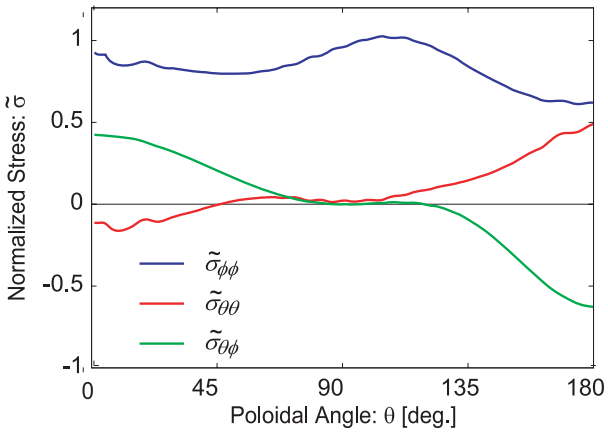

Fig. 5 Distribution of normalized stresses of torus shell without modulation by FEM. Red, blue and green lines show $\tilde{\sigma}_{\theta\theta}$, $\tilde{\sigma}_{\phi\phi}$ and $\tilde{\sigma}_{\theta\phi}$, respectively.

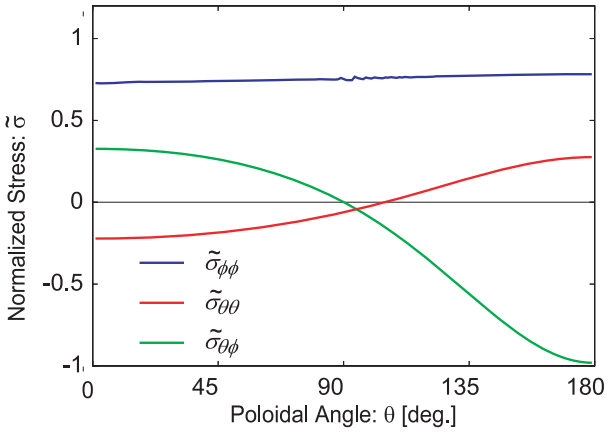

Fig. 6 Distribution of normalized stresses of torus shell without modulation by numerical integration from Eqs. (14), (15) and (17). Red, blue and green lines show $\tilde{\sigma}_{\theta\theta}$, $\tilde{\sigma}_{\phi\phi}$ and $\tilde{\sigma}_{\theta\phi}$, respectively.

4.2 Stress distribution

In order to evaluate Eq. (16), we have to numerically calculate electromagnetic forces per unit volume f_{θ}, f_{ϕ} and f_{ρ}. In this paper, we calculated electromagnetic forces by FEM analysis, and compared the results from Eqs. (14), (15) and (17) with those of FEM stress analysis.

Analysis models are axisymmetric helical coil as shown in Fig. 4, and major radius R is 2.9 m, minor radius a is 1.0 m and the thickness of the shell is 0.1 m. We calculate the stress distributions of the coil with and without modulation. The magnetic fields and electromagnetic forces are calculated from the current density, and stress distributions are given by obtained forces as loading condition by using genetic finite element method code "*COMSOL Multiphysics*". Stresses were evaluated as normalized stresses defined by

$$\tilde{\sigma}\equiv\frac{V_{\Omega}}{U_{\mathrm{M}}}\sigma, \tag{18}$$

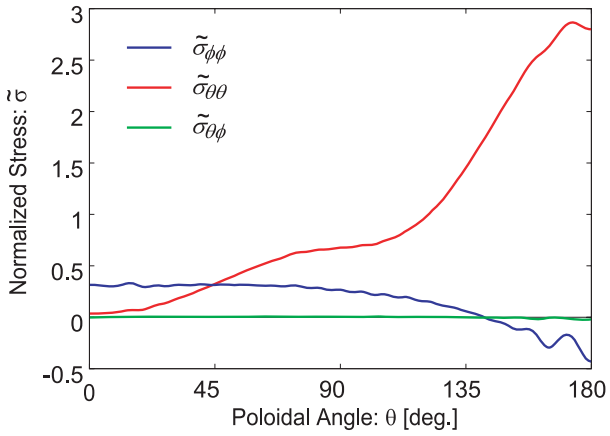

Fig. 7 Distribution of normalized stresses of torus shell with modulation by FEM. Red, blue and green lines show $\tilde{\sigma}_{\theta\theta}$, $\tilde{\sigma}_{\phi\phi}$ and $\tilde{\sigma}_{\theta\phi}$, respectively.

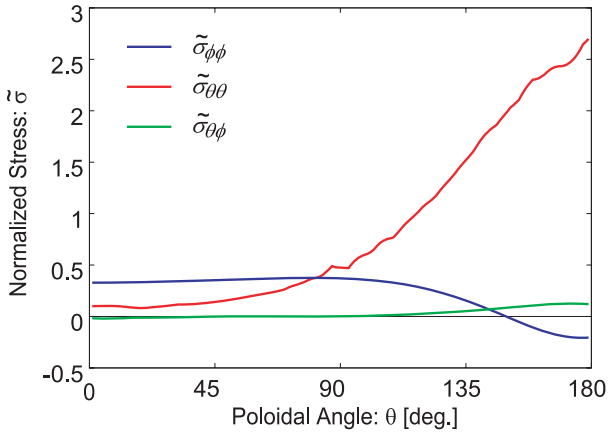

Fig. 8 Distribution of normalized stresses of torus shell with modulation by numerical integration from Eqs. (14), (15) and (17). Red, blue and green lines show $\tilde{\sigma}_{\theta\theta}$, $\tilde{\sigma}_{\phi\phi}$ and $\tilde{\sigma}_{\theta\phi}$, respectively.

where V_Ω is the volume of torus shell and U_M is the magnetic energy. Figures 5-8 show $\tilde{\sigma}_{\phi\phi}$, $\tilde{\sigma}_{\theta\theta}$ and $\tilde{\sigma}_{\theta\phi}$. Figures 5 and 7 indicate the results calculated by FEM, while Figs. 6 and 8 show those from Eqs. (14), (15) and (17). Figures 5 and 6 are the stress distributions of the coil without modulation, and Figs. 7 and 8 are those of the modulated coil.

FEM results include the stresses caused by local electromagnet forces as pinch forces, and pinch forces cause compression stress. If the structure is subjected to a compression stress, according to the virial theorem tensile stress becomes larger. Thus, FEM results are a little larger than numerically integrated results. Each dependence on the poloidal angle is almost the same.

5. Discussion and Conclusions

We evaluated the stability of toroidally modulated helical coil with circular cross section based on an axisymmetric shell current model. The configuration of the coil modulated to make a magnetic surface coincide with the coil surface is at a unstable equilibrium condition expressed by Eq. (9). Consequently, if a coil moves a little, an electromagnetic force enhances the displacement. Coils have finite length and rigidity in practice, and current distributions do not disarrange up to infinity. However, in the case of a superconducting wire, vibrations and the movements of the coil might be connected with quench. Therefore, it is important for this modulated coil to keep its orbit, the coil support at its original position will improve the performance.

We also derived the expressions of Eqs. (14), (15) and (17) from equilibrium equations. Stress distributions of the coil with torus shell configuration were calculated by integrating these equations numerically. Compared with the results of numerical integral values, FEM results are a little larger. This is presumably because the local electromagnetic force compress the coil, and thus tensile stresses become larger. When a magnetic surface generated by the helical coil intersects its coil surface, f_ϕ acts on the coil and is supported by shearing stress $\sigma_{\theta\phi}$ working on the coil.

The studies on stability and force equilibrium of non-axisymmetric helical coils is left for future work.

[1] Y. Miura, J. Kondoh and R. Shimada, *in Fusion Technology* (*Proc. 18th Eur. Symp. Karlsruhe, 1994*, Amsterdam) **2**, 957 (1995).
[2] S.Tsuji-Iio, H. Tsutsui, J. Kondoh, T. Obara, T. Yano, M. Igashira, M. Saito, M. Aritomi, H. Sekimoto, R. Takagi, M. Okamoto and R. Shimada, *Proc. 16th IAEA Fusion Energy Conf.* **3**, 685 (1997).
[3] J. Kondoh, T. Fujita, H. Tsutsui, Y. Sato, S. Tsuji-Iio and R. Shimada, Electrical Engineering in Japan **130**, 3, 39 (2000).
[4] T. Murakami, Y. Komatsu, H. Tsutsui, S. Tsuji-Iio, R. Shimada, S. Murase and S. Shimamoto, Fusion Eng. Des. **51-52**, 1059 (2000).
[5] S. Tsuji-Iio, Y. Komatsu, J. Kondoh, H. Tsutsui, T. Murakami, K. Shimada, T. Akiyama, T. Uemura and R. Shimada, *Proc. 17th IAEA Fusion Energy Conf. (2001 Edition)*, FTP-30 (2001).
[6] H. Tsutsui, T. Ito, K. Nakayama, S. Nomura, S. Tsuji-Iio and R. Shimada, Fusion Eng. Des. **66-68**, 1183 (2003).
[7] H. Tsutsui, S. Nomura, S. Tsuji-Iio and R. Shimada, Fusion Eng. Des. **75-79**, 67 (2005).
[8] S. Nomura, K. Kasuya, N. Tanaka *et al.*, T. IEE Japan **129-B**, 1311 (2009) [in Japanese].
[9] R. Shimada and H. Tsutsui, J. Plasma Fusion Res. **76**, 3, 258 (2000).
[10] H. Tsutsui, N. Kazuro, N. Shinichi, R. Shimada and S. Tsuji-Iio, IEEE Trans. Appl. Supercond. **12**, 644 (2002).